Data analysis in extended x-ray–absorption fine structure: Determination of the background absorption and the threshold energy

John J. Boland, Folim G. Halaka, and John D. Baldeschwieler
Division of Chemistry and Chemical Engineering, California Institute of Technology, Pasadena, California 91125
(Received 16 February 1983)

Two approaches for the determination of the background absorption (μ_0) in the extended x-ray–absorption fine structure (EXAFS) are presented. Both methods, experimental and computational, take advantage of the damping of the EXAFS amplitude resulting from the convolution with Gaussian functions of different widths. In the experimental method two or more spectra are collected with the use of different spectrometer slit widths, resulting in spectra of different resolutions for the same sample. In the computational approach the convolution is accomplished via a convolution algorithm. The intersection points of the resulting spectra are used to generate μ_0. At the absorption edge, the spectra intersect at a unique point, which is shown to be a measure of the threshold energy, E_0. Illustration of the two methods for background removal is given for a copper-foil sample. The computational approach is superior to the experimental method of damping the EXAFS spectra to give μ_0.

I. INTRODUCTION

Extended x-ray–absorption fine structure (EXAFS) refers to the modulations observed on the high-energy side of an x-ray–absorption edge. EXAFS has been shown to be sensitive to the local environment of the absorbing atom.[1] The EXAFS expression may be written as[2]

$$\chi(k)=-\sum_j \frac{N_j\,|f_j(k,\pi)|}{kR_j^2} e^{-2\sigma_j^2k^2} e^{-2R_j/d} \times \sin[2kR_j+\delta_j(k)]\,, \tag{1}$$

where N_j is the number of equivalent scatterers of type j at distance R_j, $f_j(k,\pi)$ is the backscattering function, $e^{-2\sigma_j^2k^2}$ is a Debye-Waller factor for thermal fluctuation and static disorder, $e^{-2R_j/d}$ is a term which accounts for inelastic scattering where d is the photoelectron mean free path, and $\sin[2kR_j+\delta_j(k)]$ is the interference term, with $\delta_j(k)$ the composite phase-shift function. k is the photoelectron wave vector defined by

$$k=[2m(\hbar\omega-E_0)]^{1/2}/\hbar\,,$$

where E_0 is the threshold energy and ω is the frequency of the x-ray photon.

In a transmission experiment, one measures $\mu(k)x=\ln(I_0/I)$, where $\mu(k)$ is the total absorption cross section, x is the sample thickness, I_0 is the incident x-ray beam intensity, and I is the intensity after the beam passes through the sample. $\chi(k)$ in Eq. (1) is actually obtained as

$$\chi(k)=\frac{\mu_e(k)-\mu_0(k)}{\mu_0(k)}\,, \tag{2}$$

where $\mu_e(k)=\mu(k)-\mu_v(k)$. $\mu_v(k)$ is a correction for absorption of x rays by electrons other than those of the edge under study and is calculated by fitting the pre-edge data to the Victoreen formula $\mu_v=a\lambda^3-b\lambda^4$, where a and b are constants and λ is the x-ray wavelength. A data set of length equal to that of the experiment is generated using the calculated parameters a and b above, and is subsequently subtracted from the experimental spectrum to give μ_e, the corrected absorption coefficient. $\mu_0(k)$ is the slowly varying background absorption of the absorbing atom in the absence of interfering neighboring atoms for the same sample thickness. It is evident that in order to compare the theoretical expression for EXAFS with experimental data, an accurate estimate of $\mu_0(k)$ is essential.

There is no standardized technique for background determination in EXAFS. Since there is no analytical expression for $\mu_0(k)$ that is adequate for all systems, the investigator must judge the points that represent the background absorption. These points, in most cases, are subsequently subjected to a cubic-spline fit to produce a data set of equal length to that of the experimental spectrum.[3] Recently, Cook and Sayers[4] introduced a set of criteria for background removal using the cubic-spline method. The above methods, however, are highly flexible and ultimately depend on the discretion of the investigator.

The EXAFS expression, Eq. (1), is written as a function of the photoelectron wave number k. The k range is dependent on the value chosen for the threshold energy E_0. Since k is a nonlinear function of E_0, the value of E_0 determines the frequency of the data in k space. Various approaches have been applied to the E_0 problem. In instances where model compounds are used, the same value of E_0 is chosen for both unknown and model compounds. Provided the compounds do not differ greatly, this method works reasonably well.[5] An alternative approach has been to vary E_0 until the peaks in the real and imaginary parts of the Fourier transform coincide.[6] This latter method, however, requires a knowledge of too many parameters to be useful in a study of unknown com-

pounds. A third approach invokes the concept of phase transferability by assuming that the phase difference between the unknown and model compound is a linear function of k and passes through the origin.[1] The value of E_0 is then varied until the best fit to such a line is obtained. Another approach has been to numerically differentiate the edge region and locate the inflection points.[7] In all of these methods the data are weighted by k^3 to minimize any error in the choice of E_0.

In the present paper we present two approaches to the problem of background removal in EXAFS. Both methods involve the convolution of the EXAFS spectrum with a Gaussian function, the width of which determines the extent of the damping in the observed spectrum. The first approach originated from the experimental observations that a low-resolution EXAFS spectrum results from increasing the spectrometer slit width. In the second method the EXAFS damping is achieved via the discrete convolution of the spectrum with a calculated Gaussian function. This latter method also gives a unique intersection at the absorption edge which is shown to correspond to the threshold energy E_0.

II. EXPERIMENTAL APPROACH

In this approach two data sets are employed for a given sample, one collected with a narrow slit width ($\sim 150\ \mu$m), while the second set is collected with a larger slit width (~ 1 mm), yielding a spectrum of lower resolution. In accordance with Eq. (1) the EXAFS modulations are damped around μ_0 and the intersection points of the two spectra are then nodal points that lie on the background absorption. This can be illustrated by considering the distribution of energies diffracted by the monochromating crystal [Si(111)] around some nominal position. In Fig. 1 this distribution (rocking curve) is plotted at 9500 eV. It is obvious that opening the slit will include more photons

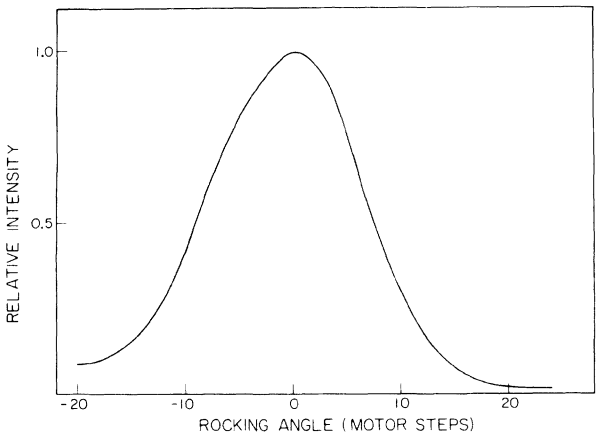

FIG. 1. Spectral distribution of energies about 9500 eV. This curve was obtained by rocking the Si(111) Johansson monochromating crystal around the Bragg angle for the diffraction of 9500-eV photons. A narrow slit (100 μm) was used such that the intensity collected from each point on the crystal has a very small angular spread. Each motor step corresponds to approximately 0.7 eV at this energy. Note that the distribution is slightly asymmetric indicating the increased bremsstrahlung flux at higher energies.

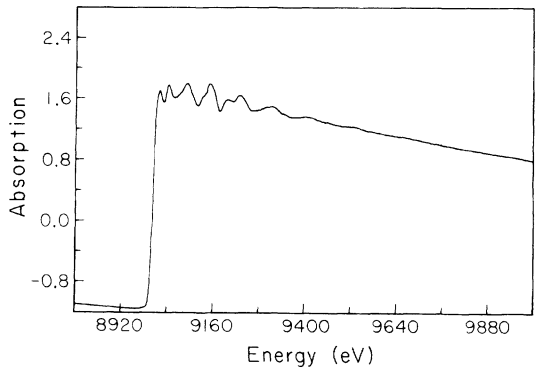

FIG. 2. Plot of the absorption vs x-ray energy for a 12.5-μm-thick copper foil. Slit width is 125 μm.

of different energies accounting for the observed damping of the EXAFS.

To illustrate this method of background removal the analysis of the EXAFS data from a 12.5-μm-thick copper foil is presented. All measurements were made at room temperature and in the transmission mode utilizing the Caltech Laboratory EXAFS spectrometer (to be described elsewhere). The energy scale of the spectrometer was calibrated by assigning the energy of the Cu $K\alpha_1$ emission line the value of 8066 eV. Figure 2 shows a plot of absorption versus energy for copper collected with a slit width of 125 μm. Preliminary data analysis involves removing the absorption due to electrons other than the K shell of copper. This is accomplished by using the Victoreen formula as discussed earlier and allows the EXAFS to be normalized as given in Eq. (2).

Figure 3(a) displays the absorption spectra of copper for slit widths of 125 μm and 1 mm. The first peak above the edge in the high-resolution spectrum is washed out when the slit is opened. Beyond this point, however, the two spectra are matched peak for peak with the amplitude of the low-resolution spectrum being noticeably damped.

It is important to note that not all intersection points in a given pair of spectra are true nodal points. This is because there are different frequency components of different amplitudes contributing to the EXAFS at each point in k space. The true isosbestic points become apparent if an additional spectrum is recorded with a third slit width as shown in Fig. 3(b) and will become more evident in Sec. III below. In practice, however, we have found that the extra intersection points lie symmetrically about the true background and contribute negligible errors if these points are included with a smoothing spline fit. The loss of the first peak after the edge is not a serious problem since a typical range for data analysis is from $k = 4$–16 Å^{-1}. To obtain the background absorption a computer program is used to calculate the difference in absorption of the two spectra in Fig. 3(a). Only those points satisfying the average difference of the two spectra in the smooth high-k region are chosen for the calculation. These points then generate the background using a cubic-spline fit with a high smoothing factor [a small smoothing factor would make the background follow the data more closely (see Cook and Sayers[4])]. The Victoreen-generated contribution to the absorption is also subtracted from this

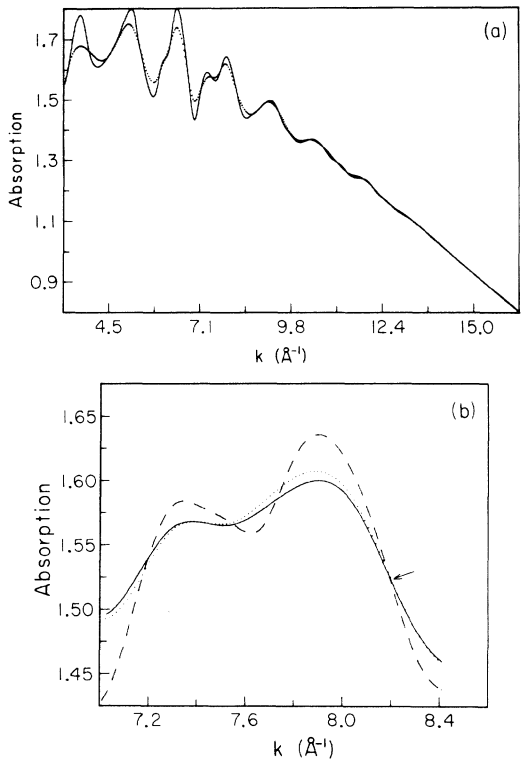

FIG. 3. Plot of the post-edge absorption vs photoelectron wave number for the copper-foil sample. E_0 was chosen to be 9004 eV (see text). (a) Solid and dotted curves refer to slit widths of 125 μm and 1 mm, respectively. (b) Dashed, dotted, and solid curves refer to slit widths of 125 μm, 1 mm, and 1.5 mm, respectively. The spectra corresponding to the two smaller slit widths intersect at four separate points in the region of k space shown. The spectrum collected with a 1.5-mm slit width intersects with only one of the above points (indicated by an arrow) and represents the only true isosbestic or nodal point.

background to give μ_0 in Eq. (2).

Figure 4 displays the post-edge absorption of the copper-foil sample versus k together with the splined background calculated as described above. Subtracting

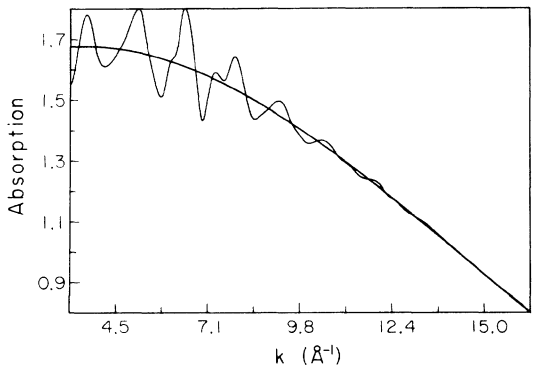

FIG. 4. Rapidly varying curve is a plot of the post-edge absorption vs photoelectron wave number for the copper-foil sample using a 125-μm slit width. Smoothly varying curve was obtained by a cubic-spline interpolation of the intersection points of the two curves shown in Fig. 3(a) and represents the background absorption.

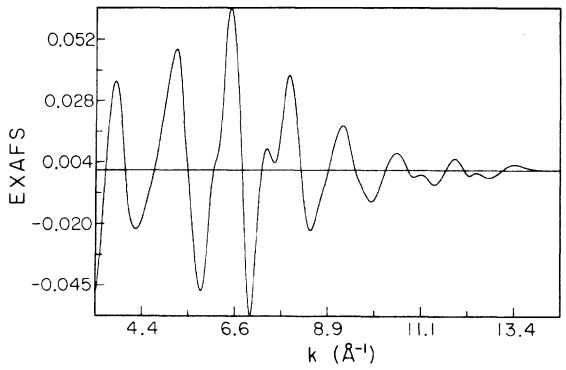

FIG. 5. Plot of $\chi(k)$ vs photoelectron wave number. Isolated EXAFS was obtained by subtracting the two curves shown in Fig. 4 and dividing the result by the calculated μ_0.

this background from the total absorption in Fig. 4 yields the desired EXAFS after dividing the difference by μ_0 (Fig. 5). Dividing by μ_0 rather than a constant is necessary if a rigorous comparison to the theoretical EXAFS expression is to be attempted. This normalization makes the EXAFS amplitude independent of the central atom and effectively weights the data more at higher k values.

The modulus of the Fourier transforms of the data shown in Fig. 5 is presented in Fig. 6. The data points were weighted by k^3, which is frequently used to balance out the approximate k^{-2} dependence of the scattering amplitude at high k and the k^{-1} factor in Eq. (1). This weighting scheme also makes the choice of E_0 less critical.

III. COMPUTATIONAL APPROACH

The experimentally observed slit function of the EXAFS spectrometer is approximately Gaussian in shape with a full width at half maximum (FWHM) of about 8 eV for a 100-μm slit width (Fig. 1). The observed damping in the EXAFS shown in Fig. 3 is the result of increasing the width of this Gaussian distribution as the slit width of the spectrometer is increased. The observed EXAFS is effectively a convolution of the true spectrum with the experimental slit function. In this section we illustrate a background-determination method which is similar to that described above except that the convolution is performed by means of a convolution algorithm.

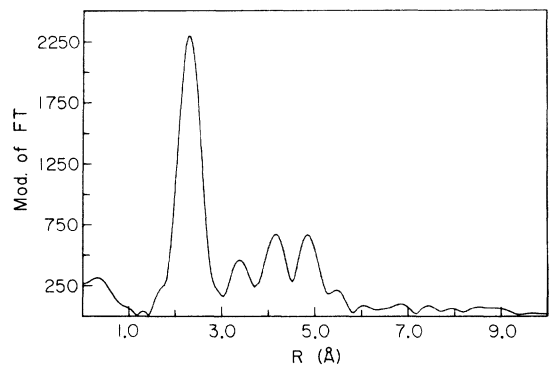

FIG. 6. Modulus of the Fourier transform for the copper-foil sample. Isolated EXAFS in Fig. 5 was weighted by k^3 as described in the text.

The convolution of a function $f(x)$ with a function $g(x)$ is defined by the convolution integral

$$h(x)=\int_{-\infty}^{\infty} f(t)g(x-t)dt \ . \tag{3}$$

For finite functions the integration limits are determined as follows: If l_1 and l_2 are the lower nonzero values of the two functions and u_1 and u_2 are their upper nonzero values, then the lower integration limit is chosen as $\max(l_1,l_2)$ and the upper integration limit as $\min(u_1,u_2)$. For large data arrays the convolution integral is readily calculated by means of the fast-Fourier-transform (FFT) and the convolution theorem. If $F(y)$ and $G(y)$ are the Fourier transforms of $f(x)$ and $g(x)$, respectively, then the convolution theorem states that the convolution integral [Eq. (3)] is the Fourier transform of the product of $F(y)$ and $G(y)$. For details on convolution, see Brigham.[8]

For the purpose of background determination, the experimentally obtained EXAFS spectrum of a 12.5-μm-thick copper foil (Fig. 2) was convolved with a series of Gaussian functions of different widths. A Gaussian distribution function was chosen in view of the shape of the observed slit function (Fig. 1). Furthermore, the smooth tails of the Gaussian distribution help minimize edge effects in the convolution process. These edge effects are similar to those seen in the Fourier filtering of peaks in distance space which gives rise to edge distortions in the back-transformed spectra. To normalize the results of the convolution to the original data the area of the slit function is set equal to 1.

Figure 7(a) illustrates the effect of convolving the experimental EXAFS (shown as dots) with a series of Gaussian functions of various slit widths. Note that the EXAFS is progressively damped as the width of the Gaussian function is increased. The intersection points of these spectra are not all unique and do not represent true isobestic points. These results are in complete agreement with the experimental observation made in Sec. II above. The effect of these convolutions on the copper absorption edge is shown separately in Fig. 7(b). The sharp rise in the edge is smeared out as the width of the Gaussian function is increased. Note that there is a unique intersection point approximately midway through the edge. This intersection point was taken to be the threshold energy E_0 (see Sec. IV). The rest of the analysis is identical to that discussed in the preceding section. Figure 7(c) shows the EXAFS plotted along with the background. Note the difference in the background absorption calculated by the two methods [Figs. 4 and 7(c)]. The k range is smaller in the computational method compared to that in the experimental method. This is due to the slight edge effect resulting from the convolution of the EXAFS with a wide Gaussian function. The distorted points in the computed convolution at high k were discarded. In addition the background determined by the computational approach does not bisect the peaks in the low-k region (below 4 Å^{-1}). The origin of this difference is the need to choose a single point that lies on the background in the low-k region where no intersection points occur due to the dominant effect of the absorption edge. This is acceptable, however, as the simple EXAFS expression, Eq. (1), is not valid beyond this range. In

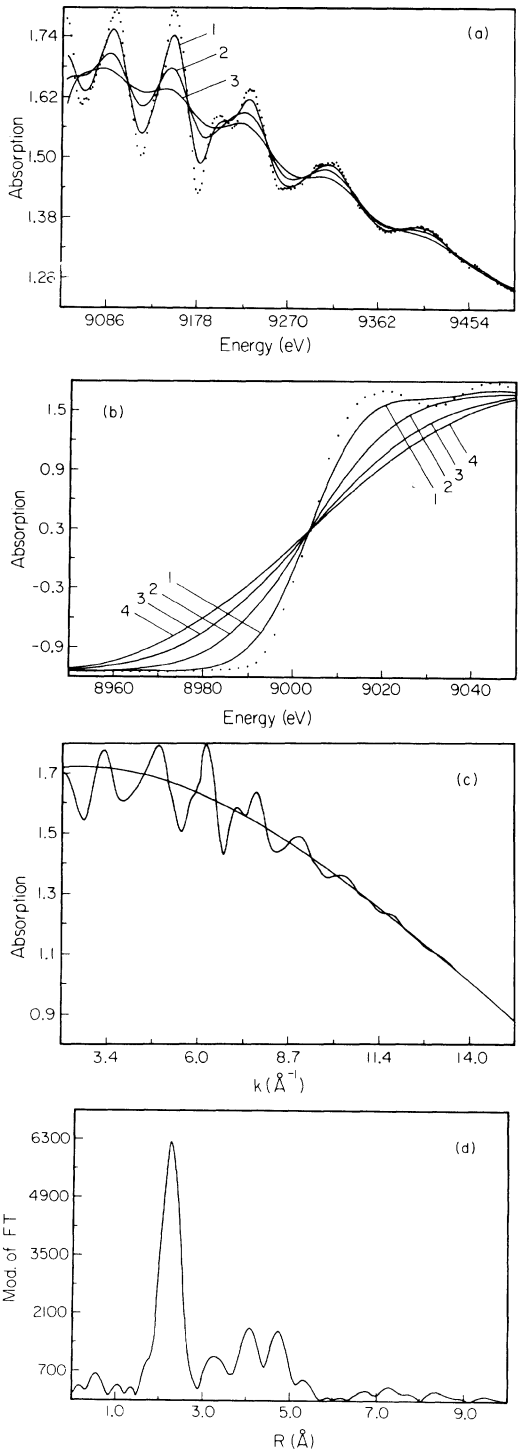

FIG. 7. (a) Plot of the post-edge absorption of the copper-foil sample vs x-ray energy. Experimental EXAFS is shown as dots. Curves 1–3 represent the convolution of the experimental EXAFS with Gaussian functions of FWHM of 16, 32, and 48 eV, respectively. (b) Effect of convolution on the absorption edge of the copper-foil sample. Experimental edge is shown as dots. Curves 1–4 represent the convolution of the absorption edges with Gaussian functions of FWHM of 16, 32, 48, and 64 eV. (c) Post-edge absorption vs photoelectron wave number for the copper-foil sample. Smoothly varying background absorption was obtained by the computational approach (see text). (d) Modulus of the Fourier transform as obtained by use of the computational approach. Compare with Fig. 6.

Fig. 7(d) the modulus of the Fourier transform is shown, and it agrees well with results obtained by other investigators.[4,9]

IV. DISCUSSION

The background-determination scheme employed above takes advantage of the fact that all EXAFS components have much higher frequencies than the background. By successively convolving the observed spectrum with a series of increasingly wider Gaussians the higher-frequency components are gradually removed. Eventually all of the EXAFS will be removed and what remains is simply the low-frequency background. This method of background determination is not very useful as serious edge effects occur due to the large widths of the Gaussian functions required to smooth out all of the EXAFS. Fortunately, however, there is a limit to the lowest-frequency EXAFS component that can exist and is determined by the smallest distance in the system. When only this lowest-frequency EXAFS component remains, increasing the width of the Guassian serves to further dampen this component. The intersection points of these dampened spectra are unique due to the presence of the single remaining EXAFS component. These points are then used to generate the background. It is important to note that the intersection points are not unique until the Gaussian function is sufficiently wide to eliminate all EXAFS other than the lowest-frequency EXAFS component.

Improper background removal in EXAFS can cause erroneous interpretation of the Fourier-transform results even for data with a high signal-to-noise ratio. In both the experimental and the computational methods described above, the Fourier transform contains structural information up to the fifth shell of copper. There is a low-amplitude peak in the (0—1)-Å region of the transform indicating a spurious low-frequency component in the isolated EXAFS. This peak is smaller for the computational method than in the experimental technique. The size and position of this peak, however, does not distort the peaks at higher R values which contain the structural information. While the magnitude of such a peak is a measure of successful background removal, it is not the only criterion that must be satisfied. It is important that the calculated background does not add or subtract frequency components which may distort the true EXAFS. This condition is necessarily fulfilled using the convolution approach described above. The transforms shown in Figs. 6 and 7(d) satisfy the empirical criteria for background subtraction set by Cook and Sayers.[4]

Other experimental methods of damping the observed EXAFS are also possible. If a variable-temperature study is made over a wide range the nodal points of these data sets may be used to generate the background absorption curve. The damping, however, is more pronounced at high k making the variable-slit method more reliable. In laboratory EXAFS systems it is also possible to vary the bias voltage on the x-ray tube and change the focus size on the anode. This method is equivalent to the variable-slit method due to the symmetry of the Johansson geometry. Frequently, however, the dynamic range of the bias voltage is too small to cause sufficient defocusing so that the variable-slit method is preferred.

The computational approach is preferred over the experimental method for various reasons. With the variable-slit method scattered radiation may present a problem so that the ratio of I/I_0 is not the same for all slit widths in a smooth region of the spectrum. Also, the experimental approach to the background removal effectively doubles the time necessary for data acquisition. Although this does not present a serious problem in the case of laboratory EXAFS systems, it may restrict the use of this method when data are collected at synchrotron facilities. Furthermore, the peak positions in the low-resolution experimental spectrum may not match those in a high-resolution spectrum if the spectrometer slit does not open symmetrically with respect to the beam.

The presence of a unique intersection point in Fig. 7(b) may be understood in terms of the theoretically predicted functional form of an x-ray—absorption edge. The absorption edge may be constructed from a series of discrete Lorentzians due to bound-state transitions. The contribution to the absorption edge due to transitions into the continuum may be described in terms of the integral of a Lorentzian weighted by the appropriate density-of-states function. This integral takes the form of an arctan function. The absorption edge, therefore, consists of a series of discrete Lorentzian functions superimposed on an arctan function.[10] The convolution process described above is normalized so that the area under each absorption curve is the same regardless of the width of the Gaussian slit function used. Since the widths of the slit functions are much greater than the width of the Lorentzian peaks describing the bound-state transitions, the convolution process is insensitive to these features. The normalization, however, constrains the convoluted spectra to pass through the inflection point of the arctan curve and thus maintains the same integrated absorption for all slit functions. The existence of a unique intersection point can be demonstrated by considering the convolution of a Gaussian function $g(x)$ of width parameter w and an arctan function $c(x)$ with a sharpness parameter s. The convolution integral is given by

$$g(x)*c(x)=\int_{-\infty}^{\infty}\exp[-(x-t)^2/w]\tan^{-1}(t/s)dt\ , \tag{4}$$

where the asterisk (*) represents the convolution of the two functions. Note that the arctangent function $c(x)$ has an inflection at $x=0$. From symmetry considerations, the value of the convolution integral, Eq. (4), is zero at this inflection point ($x=0$) and is independent of the width parameter of the Gaussian slit function. This prediction is in complete agreement with the computationally derived spectra in Fig. 7(b).

Theoretical studies[10] have shown that the inflection point of the arctan function is a good measure of the threshold energy E_0. Numerical differentiation techniques have been used to locate this inflection point.[7] In practice these methods are hampered by the presence of bound-state transitions. The convolution process, however, is insensitive to these details and provides good esti-

mates of E_0. We are presently engaged in a study involving a series of compounds with the same central atom to demonstrate the sensitivity of this inflection point to changes in oxidation state.

Advantage may also be taken of the convolution approach presented above to enchance spectral resolution. If the instrumental line shape or slit function is accurately known, a deconvolution algorithm may be used, for instance, to obtain edge structures from data collected with spectrometers that have insufficient resolving power. This is easily achieved by the use of the convolution theorem. If $f(k)$ and $g(k)$ represent the true EXAFS and the experimental slit function, respectively, then the observed EXAFS is given by

$$(S_{\mathrm{EXAFS}})_{\mathrm{observed}}=f(k)*g(k)\ . \tag{5}$$

If $(S_{\mathrm{EXAFS}})_{\mathrm{FT}}$, $F(r)$ and $G(r)$ are the Fourier transform (FT) of $(S_{\mathrm{EXAFS}})_{\mathrm{observed}}$, $f(k)$, and $g(k)$, respectively, then

$$(S_{\mathrm{EXAFS}})_{\mathrm{FT}}=F(r)G(r)\ . \tag{6}$$

Provided that $g(k)$ is known, the true EXAFS, $f(k)$, can be obtained by the Fourier transformation of $(S_{\mathrm{EXAFS}})_{\mathrm{FT}}/G(r)$.

The use of the deconvolution approach described above to improve resolution is currently being tested. This treatment would be a great advantage in laboratory EXAFS systems since a laboratory spectrometer in which, for example, a channel-cut arrangement[1] is used to improve the resolution, suffers a loss of flux which leads to a lower signal-to-noise ratio. The deconvolution method would offer an alternative that facilitates data acquisition in a reasonable length of time.

In summary, the convolution approach offers a simple and straightforward method for calculating the background absorption in EXAFS. Furthermore, a unique estimate of the threshold energy E_0 is obtained. The deconvolution approach offers the possibility of extracting information with improved resolution from experimental spectra.

ACKNOWLEDGMENTS

The support of the National Science Foundation (Grant No. CHE-81-12589) and the National Institute of Health (Grant No. GM21111-09A) is gratefully acknowledged.

[1]See, for example, P. A. Lee, P. H. Citrin, P. Eisenberger, and B. M. Kincaid, Rev. Mod. Phys. 53, 769 (1981).

[2]C. A. Ashley and S. Doniach, Phys. Rev. B 11, 1279 (1975); P. A. Lee and J. B. Pendry, Phys. Rev. B 11, 2795 (1975).

[3]T. K. Eccles, Stanford Synchrotron Radiation Laboratory Report No. 78/01 (unpublished).

[4]J. W. Cook and D. E. Sayers, J. Appl. Phys. 52, 5024 (1981).

[5]P. H. Citrin, P. Eisenberger, and B. M. Kincaid, Phys. Rev. Lett. 36, 1346 (1976).

[6]P. A. Lee and G. Beni, Phys. Rev. B 15, 2862 (1977).

[7]S. P. Cramer, K. O. Hodgson, E. I. Steifel, and W. E. Newton, J. Amr. Chem. Soc. 100, 2748 (1978).

[8]E. O. Brigham, *The Fast Fourier Transform* (Prentice-Hall, Englewood Cliffs, New Jersey 1974).

[9]G. Martens, P. Rabe, N. Schwentner, and A. Werner, Phys. Rev. B 17, 1481 (1978); F. W. Lytle, D. E. Sayers, and E. A. Stern, Phys. Rev. B 11, 4825 (1975).

[10]F. K. Richtmyer, S. W. Barnes, and E. Ramberg, Phys. Rev. 46, 843 (1934).